Two opposite hysteresis curves in semiconductors with mobile dopants

Jae Sung Lee, Shin Buhm Lee, Byungnam Kahng, and Tae Won Noh

Citation: Appl. Phys. Lett. **102**, 253503 (2013); doi: 10.1063/1.4811556
View online: http://dx.doi.org/10.1063/1.4811556
View Table of Contents: http://apl.aip.org/resource/1/APPLAB/v102/i25
Published by the AIP Publishing LLC.

Two opposite hysteresis curves in semiconductors with mobile dopants

Jae Sung Lee,[1] Shin Buhm Lee,[2,3] Byungnam Kahng,[2,a)] and Tae Won Noh[2,3,b)]
[1]*School of Physics, Korea Institute for Advanced Study, Seoul 130-722, South Korea*
[2]*Department of Physics and Astronomy, Seoul National University, Seoul 151-747, South Korea*
[3]*IBS-Center for Functional Interfaces of Correlated Electron Systems, Seoul National University, Seoul 151-747, South Korea*

(Received 17 April 2013; accepted 2 June 2013; published online 24 June 2013)

Semiconductors with mobile dopants (SMDs), which are distinct from conventional semiconductors, exhibit hysteretic current-voltage curves. The fundamental feature of this hysteresis curve is that it exhibits two oppositely rotating directions, whose origin is not clarified yet. Here, we investigate microscopic origin of the two types of curves and show that they result from the spatial inhomogeneity of the mobile dopant distribution in the SMD. In particular, we observed an abnormal modulation of the electronic energy band due to mobile dopants; lower (higher) density of dopants near a metal-semiconductor interface lead to higher (lower) conductance, whereas the conventional ionic models predict the reverse behaviors. © *2013 AIP Publishing LLC*.
[http://dx.doi.org/10.1063/1.4811556]

The successful application of semiconductor devices is attributable to their unique electrical properties, which are sensitive to the internal configuration of their dopants. Generally, dopants are assumed to be immobile. What happens if the dopants are mobile? Recent experimental research on semiconductors with mobile dopants (SMDs) such as oxygen vacancies ($V_O^{\bullet\bullet}$)[1,2] indicates that there are conductance changes due to the alteration of the internal dopant distribution in SMDs by an external electric stimulus, as illustrated in Fig. 1(a).[3] Due to this property, SMDs have received great interest for applications such as resistive switching phenoemena,[4] neuroscience,[5] and non-volatile memory devices.[6–9]

This conductance change results in a hysteretic current-voltage (I-V) curve. Many studies have reported two types of the I-V curves: the counter-figure-eight (cF8)[7,9,12] and figure-eight (F8)[6,13] directional curves, which are shown in Figs. 1(b) and 1(c), respectively. Moreover, the coexistence of both directions in a single sample has been reported.[2,11,14] To understand the origin of the two directions, several experiments and heuristic arguments have been presented. For example, Yang *et al.*[2] suggested that the cF8 and F8 curves are derived from the top and bottom Schottky interfaces, respectively. However, Shibuya *et al.*[11] hypothesized that the cF8 curve arises from $V_O^{\bullet\bullet}$ movement through conducting filaments inside the sample, whereas the F8 curve has a purely electronic origin. Subsequently, the same authors suggested that the cF8 and F8 curves originate from the respective inhomogeneous (or filamentary) and homogeneous distributions of $V_O^{\bullet\bullet}$ parallel to the interface.[14]

Despite these experimental results and heuristic arguments, the origin of the two ways of hysteretic I-V curves has not been elucidated theoretically yet. In this study, we theoretically demonstrate that the two ways of I-V hysteretic curves intrinsically appear in the SMD, resulting from the spatial inhomogeneous distribution of dopants. Interestingly, our model clearly shows that there exists an abnormal modulation of the interfacial electronic energy band when most dopants are distributed near the Schottky interface.

Conventionally, the migration of donors in an n-type semiconductor is known to cause the cF8 hysteresis curve.[2] Consider an n-type Schottky contact, as shown in Fig. 1(a). When a positive (negative) bias V_+ (V_-) is applied, the donor concentration ρ_d becomes low (high) near the interface. Then, the Schottky barrier width w_{sb} increases (decreases) because $w_{sb} \propto 1/\sqrt{\rho_d}$,[10] thus, the conductance decreases (increases) as denoted by ① (②) in Fig. 1(b). This corresponds to cF8 curve.

First of all, let us introduce a simple theoretical model in one dimension to illustrate the mechanism of the two ways in

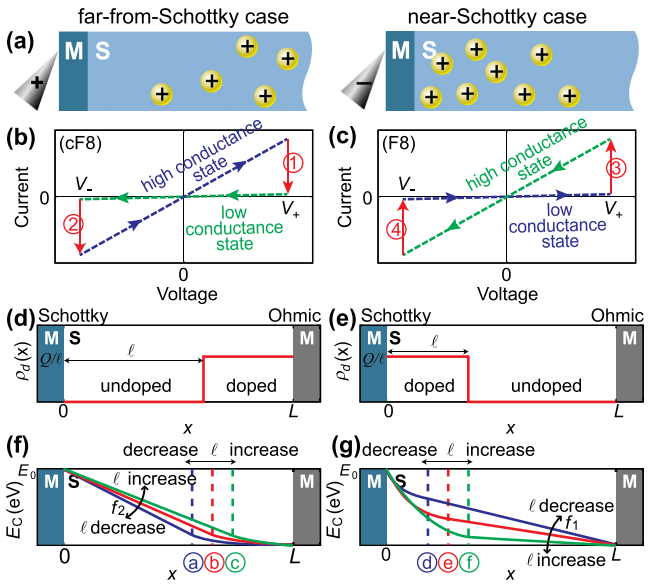

FIG. 1. (a) Schematics of a SMD. Dopants can be repelled or attracted by applying a positive or negative bias, respectively. (b) and (c) are the schematics for cF8 and F8 I-V hysteresis curves, respectively. (d)-(g) one-dimensional SMD model. (d) and (e) show the dopant density distribution $\rho_d(x)$ for the far-from-Schottky and near-Schottky cases, respectively. (f) and (g) show the effects of donor movement on the Schottky barrier for the far-from-Schottky and near-Schottky cases, respectively.

a)Electronic mail: bkahng@snu.ac.kr
b)Electronic mail: twnoh@snu.ac.kr

SMD depending on the initial dopant distribution. In this model, the semiconductor is in contact with the metals located at $x = 0$ and $x = L$ to form the Schottky and Ohmic interfaces (Fig. 1(d)) with the boundary conditions $E_C(x = 0) = E_0$ and $E_C(x = L) = 0$, respectively. We consider two different cases of initial dopant density distributions: dopants are located (i) far from (Fig. 1(d)) and (ii) near (Fig. 1(e)) the Schottky interface. For simplicity, we assume that the dopant density distribution $\rho_d(x)$ is constant in space. Then, for doped region, $\rho_d = Q/(L - \ell)$ in the region $[x = \ell, L]$ for the far-from-Schottky case and $\rho_d = Q/\ell$ in $[x = 0, \ell]$ for the near-Schottky case, where Q is the total amount of dopants in a semiconductor and assumed to be a conserved quantity. For undoped region, $\rho_d = 0$. This simplification is very useful to capture the essential mechanism of the two ways of the hysteresis curves. We assume that the electrons are fully depleted in the doped region for analytic calculation. Non-constant $\rho_d(x)$ and not-fully depleted cases will be treated numerically later. Under this simplified circumstance, the position-dependent conduction band $E_C(x)$ can then be calculated by solving the Poisson's equation,[15] $\nabla^2 E_C(x) = e\rho_{sc}(x)/\epsilon$, where e is the electronic charge, $\rho_{sc}(x)$ is the space charge density, and ϵ is the permittivity of the semiconductor. Note that $\rho_{sc}(x) = q\rho_d(x)$, where q is the dopant charge. Here, we deal with the case $q > 0$ (n-type semiconductor).

We first consider the far-from-Schottky case. The Poisson's equations for $E_C(x)$ in the regions $x < \ell$ and $x > \ell$ become $d^2E_C(x)/dx^2 = 0$ and $d^2E_C(x)/dx^2 = qeQ/\epsilon(L - \ell)$, respectively. Using the boundary conditions, $E_C(x = 0) = E_0$ and $E_C(L) = 0$, and continuity at $x = \ell$, we can easily obtain $E_C(x)$ in the whole range. Particularly for $x < \ell$, we obtain that

$$E_C(x) = f_1 x + E_0, \quad \text{where } f_1 = -\frac{E_0}{L} - \frac{qeQ(L - \ell)}{2\epsilon L}. \quad (1)$$

Here, f_1 is the slope of E_C in the undoped region. If ℓ is initially located at ⓐ in Fig. 1(f) and a positive bias V_+ is applied, ℓ increases as the direction ⓐ → ⓑ → ⓒ. Then f_1 increases or the slope in the undoped region becomes less steeper (Eq. (1)) as shown in Fig. 1(f), which makes the Schottky barrier width w_{sb} thicker. Therefore, the conductance decreases, which corresponds to the conductance change denoted by ① in Fig. 1(b). If a negative bias V_- is applied to this low conductance state, ℓ will change reversely as ⓒ → ⓑ → ⓐ. Then the conductance increases as denoted by ② in Fig. 1(b). This result agrees with the conventional explanation for cF8 curve.

For the near-Schottky case, the calculation for $E_C(x)$ can be performed similarly. The Poisson's equations for $x < \ell$ and $x > \ell$ become $d^2E_C(x)/dx^2 = qeQ/\epsilon\ell$ and $d^2E_C(x)/dx^2 = 0$, respectively. For $x > \ell$, we obtain that

$$E_C(x) = f_2(x - L), \quad \text{where } f_2 = -\frac{E_0}{L} + \frac{qeQ\ell}{2\epsilon L}. \quad (2)$$

If initial ℓ is located at ⓓ in Fig. 1(g), V_+ makes ℓ increase as the direction ⓓ → ⓔ → ⓕ. Then, by the similar explanation as the far-from-Schottky case, w_{sb} becomes thinner as shown in Fig. 1(g) and the conductance increases, which corresponds to the conductance change denoted by ③ in Fig. 1(c). If V_- is applied to this high conductance state, reverse process occurs, which causes the conductance decreases as denoted by ④ in Fig. 1(c). Therefore, this result verifies that F8 curve intrinsically appears in SMD without the assumption of the electronic function or the two Schottky interfaces.

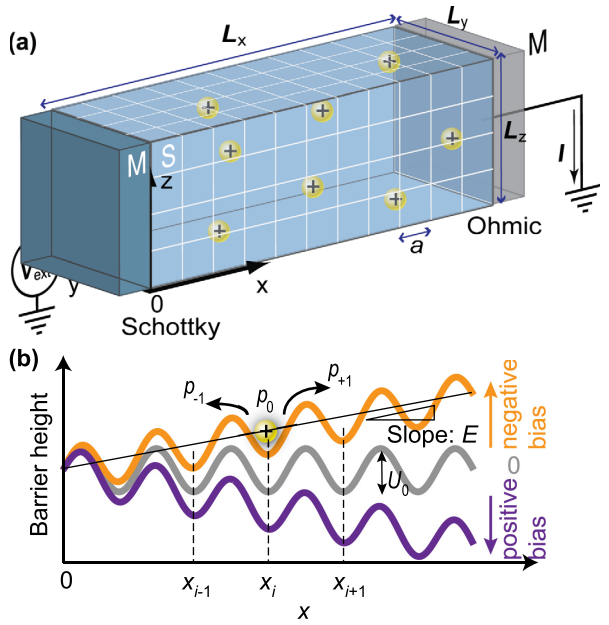

FIG. 2. (a) Configuration of the simulation. Donors are denoted by yellow circles. (b) Periodic potential energy of the donors, where local minima correspond to the lattice sites. Grey, orange, and purple curves denote the periodic potential energies when V_{ext} is zero, negative, and positive, respectively. U_0 is the energy barrier height against the movement of a donor. Donors move according to the hopping probabilities p_0, p_{+1}, and p_{-1} (Eq. (3)).

Now, using numerical simulations, let us generalize the above analysis in three dimension without the assumptions of uniform $\rho_d(x)$ and fully depleted doped region. For quantitative calculation, we use the parameters for Pt-$SrTiO_3$ contact. Let us consider a three-dimensional lattice (lattice constant $a = 0.39$ nm) whose lengths in x-, y-, and z-directions are L_x, L_y, and L_z, respectively, as shown in Fig. 2(a). Here, $L_x = L_y = L_z = 27.3$ nm for manageable calculation. Two different metals are in contact with the lattice at $x = 0$ and $x = L_x$ forming Schottky and Ohmic contacts, respectively. Donors ($V_O^{\bullet\bullet}$) were distributed on the lattice depending on $\rho_d(x)$.

Then the position-dependent conduction band $E_C(x_i, y_j, z_k)$ can be calculated numerically by solving the Poisson's equation, $\nabla^2 E_C(x_i, y_j, z_k) = e\rho_{sc}(x_i, y_j, z_k)/\epsilon$. However, the calculation of E_C is not straightforward because $\rho_{sc}(x) \neq q\rho_d(x)$. Therefore, we use the self-consistent relaxation method to obtain ρ_{sc} and E_C simultaneously; we divide ρ_{sc} into two parts: $\rho_{sc} = \rho_+ - \rho_-$, where ρ_+ and ρ_- are the densities of positive and negative charges, respectively. Let us focus on highly electron-doped semiconductors, where the density of donors is sufficiently high compared with the hole density. Then $\rho_+ \approx q\rho_d(x)$. $\rho_-(x_i, y_j, z_k)$ corresponds to the density of electrons and is determined by the following equation:[10] $\rho_-(x_i, y_j, z_k) = 2N_c/\sqrt{\pi}\int_0^\infty d\eta\,\eta^{0.5}/(1 + \exp[\eta - \beta\{E_F - E_C(x_i, y_j, z_k)\}])$, where β is the inverse temperature and N_c is the effective density of the states in the conduction

band. In this simulation, we used $N_c = 2.5 \times 10^{19}\,\mathrm{cm}^{-3}$: however, we also confirmed that the essential feature of the simulation is not changed by variation of N_c. Note that we set $E_F = V_{\mathrm{ext}}$, where V_{ext} is applied voltage between two electrodes, and assume that the barrier height at the interface is independent of the dopant density.[13] Thus, we can set up the boundary conditions at $x=0$ (ideal Schottky) and $x=L_x$ (ideal Ohmic) interfaces as $E_C(0,y,z) = 0.9$ eV (Ref. 16) and $E_C(L_x,y,z) = V_{\mathrm{ext}}$, respectively. Here, we neglect the small image-charge effect due to large ϵ for $SrTiO_3$. Inserting $\rho_+(x_i,y_j,z_k)$ and $\rho_-(x_i,y_j,z_k)$ into the Poisson's equation, we obtain $E_C(x_i,y_j,z_k)$ and $\rho_{sc}(x_i,y_j,z_k)$ simultaneously. To confirm the validity of this technique, we calculate $E_C(x_i,y_j,z_k)$ for a silicon semiconductor with various doping concentrations. The results are presented in supplemental material (SM), section 1.[21]

Next, using the obtained $E_C(x_i,y_j,z_k)$, the electric current I of the major carriers (i.e., electrons) can be estimated with the following formula:[17]

$$I = \sum_{j,k} \frac{4e\pi m_e}{\beta h^3} \int_0^\infty dE_x P_{j,k}(E_x) \ln\left(\frac{f(\xi - E_x)}{f(\xi - E_x - V_{\mathrm{ext}})}\right),$$

where m_e is the free electron mass, h is Planck's constant, $\xi = \max(E_F - E_C)$, and $f(x) = 1 + e^x$. $P_{j,k}(E_x)$ is the transition probability that an electron with x-directional energy E_x will tunnel through the Schottky barrier at $y = y_j$ and $z = z_k$. In the discrete lattice, $P_{j,k}(E_x)$ can be written as $P_{j,k}(E_x) \approx \exp\left(-\alpha \sum_i a\sqrt{E_C(x_i,y_j,z_k) - E_x}\right)$, where the summation index i extends over all cases satisfying $E_C(x_i,y_j,z_k) > E_x$ and $\alpha = 1.025\,\mathrm{eV}^{-0.5}\mathrm{\AA}^{-1}$. Note that this formula includes the contributions from the thermionic emission as well as the field emission.

We assume a simple hopping motion of $V_O^{\bullet\bullet}$ along the x-direction for the donors under a periodic potential with a barrier height U_0, as shown in Fig. 2(b). We also assume that a constant electric field $E = -V_{\mathrm{ext}}/L_x$ is formed throughout the semiconductor. The validity of the constant E-field approximation is discussed in SM section 2.[21] Thus, when a negative (positive) V_{ext} is applied, the periodic potential energy for the donors increases (decreases) with a slope of E, as shown in Fig. 2(b). Then, the heights of the left and right energy barriers, compared to the local minimum, become approximately $U_0 - aE/2$ and $U_0 + aE/2$, respectively. The probability of remaining at the original site x_i (p_0) is given by the probability that the donor cannot overcome a lower barrier among the two. So, $p_0 = 1 - \exp(-\beta(U_0 - a|E|/2))$. When $V_{\mathrm{ext}} > 0$, the probability of moving to site x_{i-1} (p_{-1}) is the half of the probability that the donor overcomes the left or higher barrier. Another half of the probability should be counted for moving to the opposite direction. So, $p_{-1} = 0.5\exp(-\beta(U_0 + a|E|/2))$. By combining all of the similar terms, we obtain

$$\begin{aligned} p_{+1} &= 0.5e^{-\beta U_0}[e^{\beta|E|a/2} + 2\mathrm{sgn}(V_{\mathrm{ext}})\sinh(\beta|E|a/2)], \\ p_{-1} &= 0.5e^{-\beta U_0}[e^{\beta|E|a/2} - 2\mathrm{sgn}(V_{\mathrm{ext}})\sinh(\beta|E|a/2)], \\ p_0 &= 1 - e^{-\beta(U_0 - |E|a/2)}, \end{aligned} \quad (3)$$

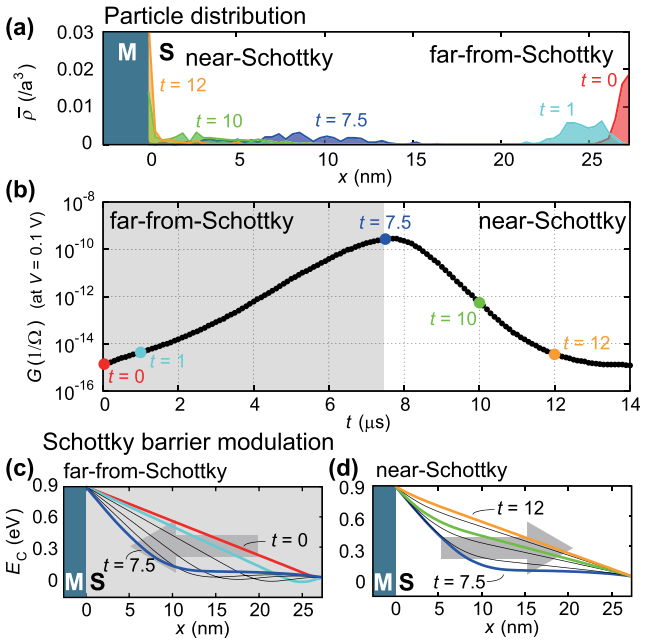

FIG. 3. (a) Changes in the donor density distribution from $t=0$ to 14 μs when a negative bias is applied. (b) Changes in the conductance as a function of time. (c) and (d) show changes of the Schottky barrier when most donors are distributed in the far-from-Schottky and near-Schottky regions, respectively. In all figures, red, cyan, blue, green, and gold are used to represent data collected at $t=0$, 1, 7.5, 10, and 12 μs, respectively.

where $\mathrm{sgn}(x) = -1$, 0, and 1 when $x < 0$, $x = 0$, and $x > 0$, respectively. For simplicity, we consider only a hardcore repulsion interaction between the two donors.

Here, we adopted the thermal acceleration mechanism[18] applied for $SrTiO_3$, which takes into account the Joule heating effect to reproduce the experimentally observed fast-switching time ($\sim 10^{-6}$ s). So, high temperature $\beta \sim 15\,\mathrm{eV}^{-1}$ (800 K) can be used for hopping with $U_0 = 1.01$ eV.[18] Note that our simulation results based on this constant-high-temperature assumption essentially do not change, even though we take into account temperature change due to variations in the external voltage. Here, the attempt frequency for the hopping is 10^{13} Hz.[19]

Using the above equations, we simulated the case in which the donors move from the Ohmic to the Schottky interface. Initially, the donors were uniformly distributed with a density of 10^{19} /cm^3.[18] Using Eq. (3), we pushed the donors toward the Ohmic interface by applying a positive bias, the red curve in Fig. 3(a). Then, we applied a negative voltage $V_{\mathrm{ext}} = -1.875$ V to attract donors towards the Schottky interface. Here, the donor density at x_i is defined as $\bar{\rho}(x_i) \equiv n(x_i)/(L_y L_z)$, where $n(x_i)$ is the number of donors at the $x = x_i$ plane. Here, $\epsilon = 100\epsilon_0$ (Ref. 20) in high electric field (ϵ_0 is the permittivity in free space), with periodic boundary conditions in the y- and z-directions. Fig. 3(a) shows the time-dependent distribution of the donors. The distribution moved toward the Schottky interface over time.

The conductance $G(\equiv I/V_{\mathrm{ext}})$ during the attraction process is calculated at 0.1 V as a function of time t. As indicated in Fig. 3(b), the G-t plot can be divided into two regions: for $t < 7.5$ μs, G increases as a function of t, and for $t > 7.5$ μs, G decreases. When comparing the distributions shown in Fig. 3(a), G increased (decreased) when most

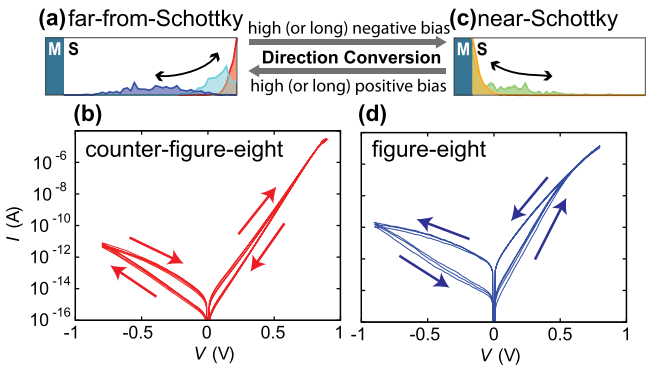

FIG. 4. If the donors are initially distributed in the far-from-Schottky region (a), the voltage sweep results in a cF8 *I-V* curve (b). If the donors are initially distributed in the near-Schottky region (c), a F8 curve (d) is obtained. By applying a large negative bias to the lattice exhibiting a cF8 direction, we can attract donors into the near-Schottky region, and then the direction of *I-V* curve will change to F8 way. The opposite effect can be obtained by applying a large positive bias.

dopants were distributed in the far-from-Schottky (near-Schottky) region.

The two different t-dependences of G come from the different modulation behaviors of the Schottky barrier during the attraction process. For each t, we obtained $E_C(x_i)$ by calculating $E_C(x_i, y_j, z_k)$ at $V_{\text{ext}} = 0$ and averaging over y_j and z_k. Fig. 3(c) shows $E_C(x_i)$ when most dopants were distributed in the far-from-Schottky region (i.e., $t < 7.5\,\mu$s). In this case, the pulling of the donors toward the Schottky interface resulted in a decrease in the Schottky barrier width, and G increased. Fig. 3(d) presents the case $E_C(x_i)$ where most dopants were distributed in the near-Schottky region (i.e., $t > 7.5\,\mu$s). In this case, the attraction of the donor increased the Schottky barrier width rather than decreasing it. These results agree with those of the one-dimensional SMD model.

We also simulated *I-V* curves under a repetitive voltage sweep, with different initial donor distributions. Here, it took 0.1 μs for each voltage point and voltage gap is 0.027 V. When most donors were initially distributed in the far-from-Schottky (near-Schottky) region as shown in Fig. 4(a) (Fig. 4(c)), cF8 (F8) curve is generated as shown in Fig. 4(b) (Fig. 4(d)), which corresponds to the direction of Fig. 1(b) (Fig. 1(c)). Furthermore, the direction of the *I-V* curve can be changed by applying a large bias, as indicated in Fig. 4.

In conclusion, we introduced the SMD model which demonstrates that two opposite hysteresis curves intrinsically appear in the SMD due to the inhomogeneous dopant density distribution. From this theoretical analysis, we can control the type of the *I-V* curve by modulating the mobile dopant distribution. The theoretical result we obtained in the letter may become a fundamental basis for further development of SMD.

This research was supported by the National Research Foundation of Korea, Grant Nos. 2010-0015066 (B.K.) and Nos. NRF-2011-35B-C00014 (J.S.L.) and by the Research Center Program of Institute for Basic Science [Grant No. EM1203] in Korea (T.W.N).

[1]R. Waser and M. Aono, Nature Mater. **6**, 833–840 (2007).
[2]J. J. Yang, J. Borghetti, D. Murphy, D. R. Stewart, and R. S. Williams, Adv. Mater. **21**, 3754–3758 (2009).
[3]D. B. Strukov, G. S. Snider, D. R. Stewart, and R. S. Williams, Nature **453**, 80–83 (2008).
[4]R. Waser, R. Dittmann, G. Staikov, and K. Szot, Adv. Mater. **21**, 2632–2663 (2009).
[5]D. B. Strukov, Nature **476**, 403 (2011).
[6]J. J. Yang, M. D. Pickett, X. Li, D. A. A. Ohlberg, D. R. Stewart, and R. S. Williams, Nat. Nanotechnol. **3**, 429–433 (2008).
[7]M. Janousch, G. I. Meijer, B. Delley, S. F. Karg, and B. P. Andreasson, Adv. Mater. **19**, 2232–2235 (2007).
[8]Y. B. Nian, J. Strozier, N. J. Wu, X. Chen, and A. Ignatiev, Phys. Rev. Lett. **98**, 146403 (2007).
[9]M.-J. Lee, C. B. Lee, D. Lee, S. R. Lee, M. Chang, J. H. Hur, Y.-B. Kim, C.-J. Kim, D. H. Seo, S. Seo *et al.*, Nature Mater. **10**, 625–630 (2011).
[10]S. M. Sze and K. K. Ng, *Physics of Semiconductor Devices*, 3rd ed. (Willey, New Jersey, 2007), Chap. 1.
[11]K. Shibuya, R. Dittmann, S. Mi, and R. Waser, Adv. Mater. **22**, 411–414 (2010).
[12]K. Szot, W. Speier, G. Bihlmayer, and R. Waser, Nature Mater. **5**, 312–320 (2006).
[13]D. S. Shang, J. R. Sun, L. Shi, and B. G. Shen, Appl. Phys. Lett. **93**, 102106 (2008).
[14]R. Muenstermann, T. Menke, R. Dittmann, and R. Waser, Adv. Mater. **22**, 4819–4822 (2010).
[15]D. A. Neamen, *Semiconductor Physics and Devices Basic Principles*, 3rd ed. (McGrawHill, New York, 2003), Chap. 9.
[16]J. Robertson and C. W. Chen, Appl. Phys. Lett. **74**, 1168 (1999).
[17]R. Straton, J. Phys. Chem. Solids **23**, 1177–1190 (1962).
[18]S. Menzel, M. Waters, A. Marchewka, U. Böttger, R. Dittmann, and R. Waser, Adv. Funct. Mater. **21**, 4487–4492 (2011).
[19]S. H. Jeon, W.-J. Son, B. H. Park, and S. Han, Appl. Phys. A **102**, 909–914 (2011).
[20]R. A. van der Berg, P. W. M. Blom, J. F. M. Cillessen, and R. M. Wolf, Appl. Phys. Lett. **66**, 697 (1995).
[21]See supplementary material at http://dx.doi.org/10.1063/1.4811556 for the calculation of the Schottky barrier for a silicon semiconductor with various dopping concentrations using the self-consistent relaxation method.